Iranian Journal of Materials Forming 8 (1) (2021) 14-25

Online ISSN: 2383-0042

IJMF

Iranian Journal of Materials Forming

Journal Homepage: http://ijmf.shirazu.ac.ir

Research Article

Study on Manufacturing of Internal Gear by Flowforming Process and Investigation of Effective Parameters on Process Force

M. Khodadadi, Kh. Khalili* and A. Ashrafi

Department of Mechanical Engineering, University of Birjand, Birjand, Iran

ARTICLE INFO

Article history:

Received 20 July 2020
Reviewed 5 October 2020
Revised 20 October 2020
Accepted 31 October 2020

Keywords:

Flowforming
Internal gear
Finite element analysis
Design of experiments
Optimization

ABSTRACT

Flowforming is a plastic deformation process that is used to produce precise thin-walled tubes. Manufacturing of an internal gear through flowforming process is a new method by which the gear can be manufactured in just one pass. In the present study, the flowforming of internal gear is studied both experimentally and numerically. A simple set up was designed and built to manufacture the internal gear. The plastic behavior of the material was determined through tensile testing, and the friction condition was determined using a friction test. Parameters including profile and teeth height were measured and compared with simulated values. It is shown that there is a good agreement between the results of the simulation and those of the experiment. When the simulation is verified, the design of the experiment method is employed to investigate the influences of roller diameter, feed rate, thickness reduction percentage and attack angle on the process force. According to DOE results, all parameters and interactions are significant and affect the process force except D×T. The process force increases by increasing the roller diameter, thickness reduction percentage and feed rate, but decreases by increasing the attack angle.

© Shiraz University, Shiraz, Iran, 2021

1. Introduction

Flowforming is an incremental forming technique which is used to manufacture seamless tubes with high precision and surface quality [1]. The process involves the feeding motion of one or more rollers against a metal blank or tube rotating together with the main spindle of a machine to obtain desired axisymmetrical and hollow geometries by inducing continuous and localized plastic deformation on the blank or tube [2]. To avoid deflection of long and thin tubes, modern flow forming machines employ two or more rollers. The advantages of the process include low production cost, finer microstructure and a reduction in material waste making it suitable for automotive and aerospace industries [1].

Traditional spinning technology has been used only for manufacturing axisymmetric, circular cross-section and uniform wall-thickness parts, and the use of the technology to manufacture axisymmetric, circular cross-section, and uniform wall-thickness parts remained a challenge. One aspect of such a challenge is the manufacturing of internal gears. Currently, machining is the main method to produce internal gears, while in general, machined gears have lower strength compared to forged or rolled ones. In addition, machining is a metal removal process in which material is highly wasted especially when it comes to producing internal gears. To overcome the aforementioned drawbacks, flowforming is used in gear manufacturing [3].

* Corresponding author
E-mail address: kkhalili@birjand.ac.ir (K. Khalili)
https://doi.org/10.22099/ijmf.2020.37889.1162

Published by Shiraz University. This is an open access article under the CC BY-NC-ND license (http://creativecommons.org/licenses/by-nc-nd/4.0/).

Few finite element analyses are found that study the process. Groche and Fritsche [4] investigated gear manufacturing using flowforming. They investigated the influence of the number of rollers on the force applied to the mandrel teeth. By increasing the number of rollers, the force on the mandrel teeth acts in opposite directions, which increases the lifespan of the tool. Jiang, et al.[5-8] studied the manufacturing of thin-walled tubes including internal teeth using a ball spinning process. They studied the influences of roller diameter, feed rate and thickness reduction on teeth height, surface roughness and microstructure of the tube. By increasing the roller diameter, thickness reduction and feed rate, the teeth height increases. Additionally, increasing the roller diameter, improves the surface roughness. Haghshenas et al. [9-11] investigated the influences of microstructure, thickness reduction percentage and strain hardening rate on the plastic strain in metals with FCC structure. Plastic strain in the workpiece rises by increasing the thickness reduction percentage and strain hardening rate. Xia et al. [12] analyzed Trapezoidal internal gear production defects, experimentally and numerically. They examined the effect of thickness reduction and direction of rotation of the mandrel on the shape of the gear. The greater the thickness reduction in the first pass, the more uniform the shape of the gear. Xu et al. [13] studied, both experimentally and numerically, the multi-stage internal gear production using a plate. They investigated the effect of process parameters on the tooth height and filling rate of the mandrel cavity. The process was applied to ASTM 1035 mild steel using three rollers in two stages. By increasing the thickness reduction, the initial thickness and the feed rate, the filling rate increases uniformly.

Although the process has received attention from the research community, some aspects of the process has not been studied yet. Predicting the amount of required force or power is very important to choose equipment and tools that are suitable for the process. Moreover, an important advantage of this process is a low forming force compared to other forming processes. Therefore, investigation of the process force is very important. Moreover, the influence of parameters has not been studied so far. The present study describes the simulation of internal gear flowforming process performed on a tube made of copper. Finite element method is employed to analyze the process. Experiments were designed and carried out to manufacture the part. In the present study, the emphasis is on investigating the influence of process parameters on process force in backward flowforming of internal gears using the results of experiment and FEM.

2. Experiments

To obtain the mechanical properties of the sample, tensile testing was done at room temperature and higher temperatures. Then, the ring pressure and friction were tested. Finally, the flowforming process was carried out on the workpiece.

2.1. Tensile test

In the process of flowforming, temperature rises and shifts the stress-strain diagram. Thus, it is necessary to determine the plastic behavior of the workpiece regarding an increased temperature. The tensile test is employed to determine the plastic behavior of the material. The test was carried out on a Zwick/Roell tensile test machine with a maximum load of 650 kN with a servo motor control. Test samples were prepared according to the ASTM E8. The tests were carried out in temperatures of 25, 100 and 150 degrees Celsius with a rate of 20 mm/min. The obtained stress-strain diagrams are presented in Fig. 1.

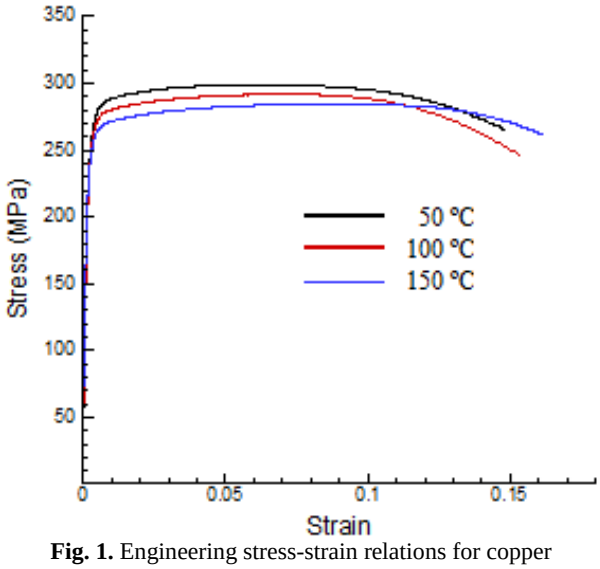

Fig. 1. Engineering stress-strain relations for copper workpiece.

2.2. Friction test

Because the temperature increases during the flowforming process and given that it influences the friction coefficient, the test was carried out in temperatures of 25, 60, 100, and 150 degrees Celsius. The test samples were rings with a standard geometrical ratio of 2:3:6 (thickness of 8 mm, an internal diameter of 12 mm and an external diameter of 24 mm). Fig. 2 presents the ring pressure sample and its dimensions. A Zwick/Roel pressure test machine, which is presented in Fig. 3, with a maximum load of 650 kN was used to carry out the tests. The final dimensions of the samples were measured after the results of the tests and the friction coefficient was determined.

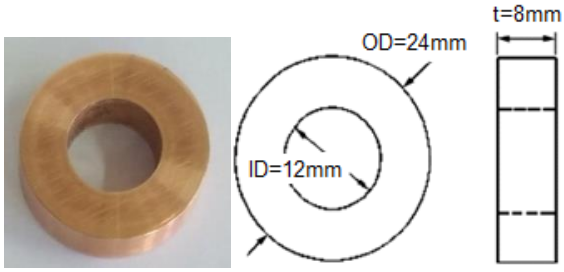

Fig. 2. Dimensions of ring pressure test sample.

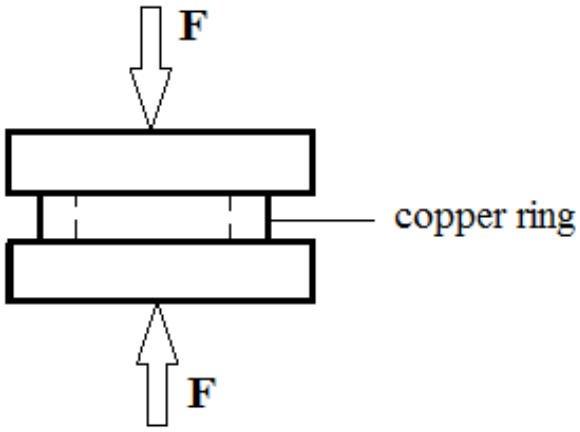

Fig. 3. Schematic of ring pressure test.

2.3. Flowforming process

In this study, a backward flowforming process was performed using a universal lathe machine. An AISI 1045 mandrel and a ball-bearing as the roller were used. A gear with 20 teeth and an outer diameter of 13.2 mm which was heat treated to get the surface hardness of 58 RC was used as the mandrel (Fig. 4). The roller was a deep groove ball-bearing SKF 6203/VA201 with a diameter of 40 mm and a width of 12 mm. The roller was installed on the transverse support of the lathe machine. The preform was a C12200 copper alloy tube with an internal diameter of 13.2 mm and a wall thickness of 2.5 mm (Fig. 5). The process preparation includes machining to size the preform, some surface cleaning and initial lubrication of the contact surface of the mandrel and the preform. The spinning was performed at 500 rpm spindle speed. The experiment setup is shown in Fig. 6. The gear was completed in four passes of forming, where the thickness was reduced and the gear tooth was formed in each step. The thickness reduction ratio is stated as a percentage of the preform thickness. The minimum thickness reduction should be determined so that the plastic metal flow would not be limited to the external surface, which is usually 15% [14]. The primary preform was removed from the mandrel when 25% thickness reduction was achieved. This was repeated in the second step, i.e., a 25% thickness reduction was also carried out in the second step. In the third step, the thickness reduction was 20%, and in the fourth step 15%. To evaluate the gear teeth, it was necessary to section the specimens, which was done using a wire-cut machine. A video measuring machine (VMM) was used to measure the profile and height of gear teeth in the sectioned specimens.

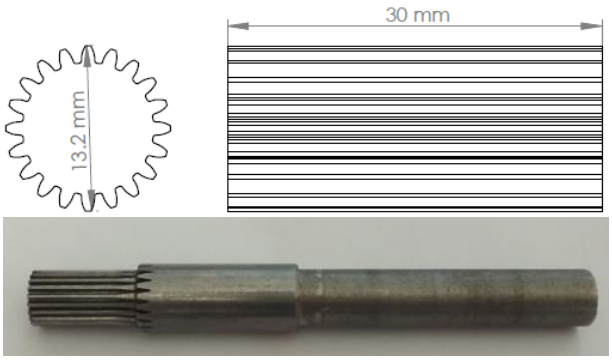

Fig. 4. Mandrel used to form internal gear.

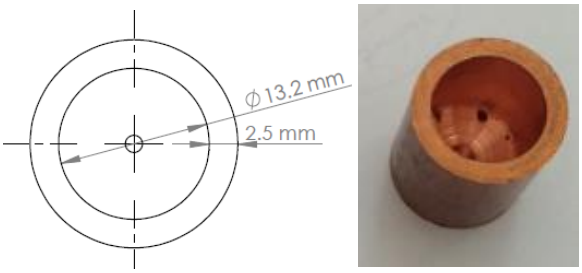

Fig. 5. Dimensions of preform.

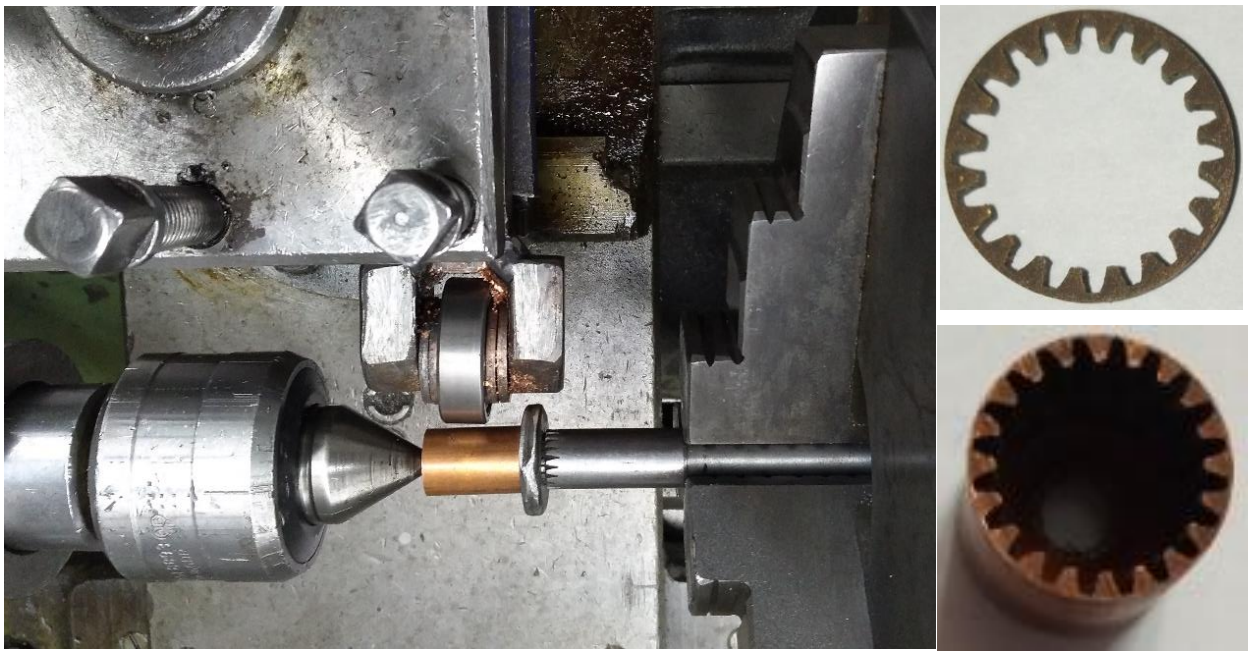

Fig. 6. Setup of the experiment and the produced final gear.

3. Modeling of Flowforming Process

In this study, the workpiece material was C12200 copper alloy with the mechanical properties shown in Fig. 1. A thermo-mechanical analysis was carried out and 41470 C3D8RT type elements were used for meshing. For simplicity, the mandrel and the roller were considered to be rigid. The model is shown in Fig. 7. The Coulomb friction model was used to define the contact surfaces, and the friction coefficient was determined according to the friction test (which was described in Subsection 2.2). The dynamic explicit solving procedure was used, and then, the mass scaling factor was utilized to reduce the solution time. Given that the temperature rises during the process due to friction, thermal contact property and surface film conditions were defined. Because of severe and non-homogeneous plastic deformation of the workpiece, meshes may experience severe distortion resulting from decreased solving precision and steady-state deformation, which may even stop problem-solving. To overcome this, the arbitrary Lagrangian-Eulerian (ALE) formulation was used. In this approach, elements can move independent of the material and are not pure Lagrangian, i.e., navigating spatially, nor pure Eulerian, i.e., fixed spatially. Instead, they move spatially together with the material while the material can also flow through their boundaries [15]. The analysis and simulation were performed in FE software environment.

4. Statistical Optimization

A lower required load is an advantage of this process compared to other ones, thus, investigating the influence of each parameter on the process force is necessary. The response surface method (RSM) was used to investigate the effect of each parameter on the process force. The response surface method is a statistical method that is used to model and analyze processes, affected by several parameters. The goal of this method is modeling and optimization of the response [16]. In this study, the central composite design (CCD) was applied. In this process, four parameters including roller diameter, thickness reduction percentage, feed rate, and attack angle (as shown in Fig. 9) are more important than others [17]. The levels of these parameters are given in Table 1. According to the applied method, 31 experiments were considered using the software with α=2.

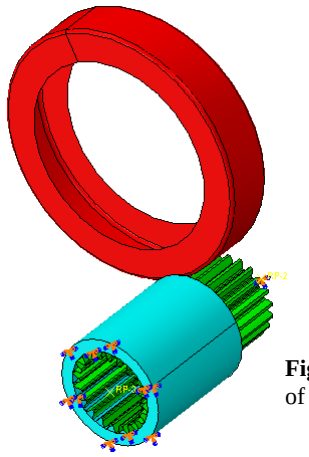

Fig. 7. Simulation procedure of flowforming process.

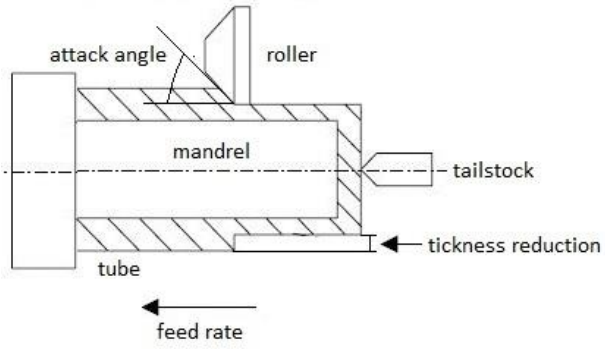

Fig. 8. Effective parameters in flowforming process [17]

Table 1. Effective parameter and their levels

parameter	Roller diameter(D)	Thickness reduction percentage (T)	Feed rate(f)	Attack angle(α)
Low level	20 mm	15%	0.05 mm/rev	20 (degree)
High level	60 mm	35%	0.25 mm/rev	60 (degree)

5. Results

In this section, the experimental and simulation results are discussed, and the influence of the parameters on the process force and statistical optimization is found.

5.1. Experimental and simulation results

The manufacturing of the gear was carried out in four steps and the gear teeth were formed gradually. Fig. 9 presents the form and height of the gear tooth, which was obtained from the simulation. The formed gear tooth in the first step, after thickness reduction by 25%, is presented in Fig. 10. Fig. 11 shows the gear tooth height after the first step in both the experimental and the simulated procedure. In the second step, the gear tooth height increased as a result of thickness reduction by 25%, which is presented in Fig. 12. Fig. 13 presents the height difference in the experimental and simulation procedure. Fig. 14 shows the formed gear tooth in the third step, and Fig. 15 depicts the difference in experimental and simulation results in this step. In the fourth step, the final profile of the gear tooth was formed, and the result is presented in Fig. 16. Fig. 17 shows a comparison between the final profile and the height of the gear tooth. As can be seen, there is a good agreement between experimental and simulation results so that the maximum difference in height of the gear tooth is about 9% when the simulation is compared with experiments.

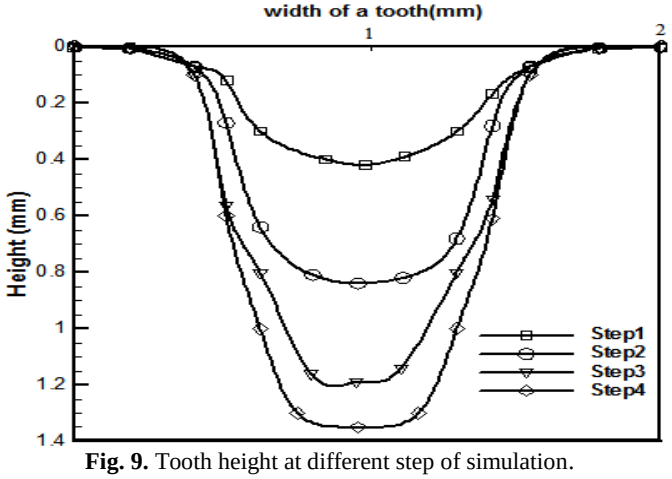

Fig. 9. Tooth height at different step of simulation.

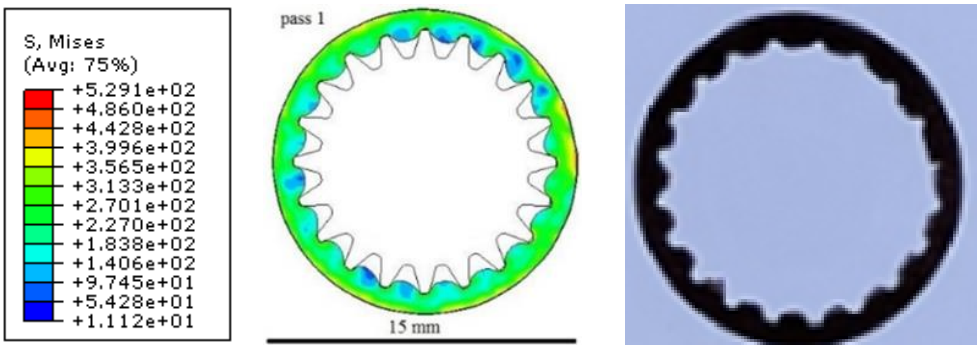

a b c

Fig. 10. Tooth formation in the first step, a) Mises stress b) simulation c) experiment.

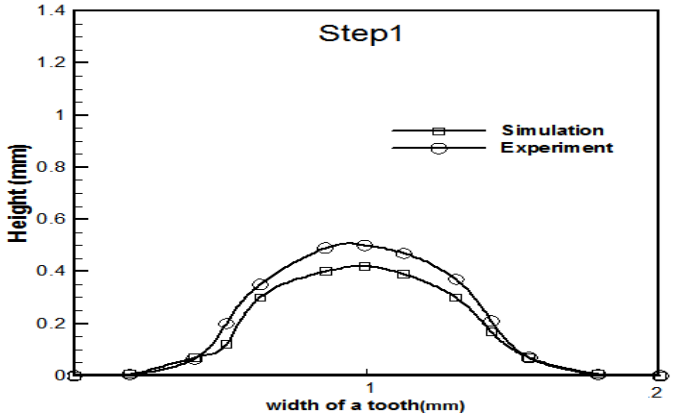

Fig. 11. Tooth shape and height in the first step in both experimental and simulation procedure.

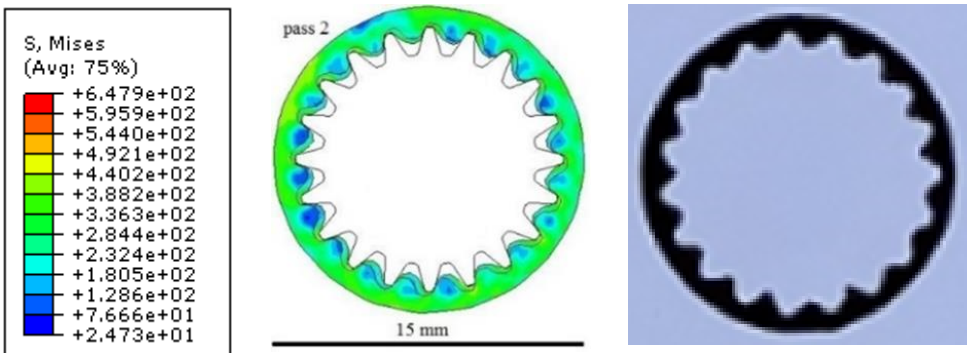

a b c

Fig. 12. Tooth formation in the second step, a) Mises stress b) simulation c) experiment.

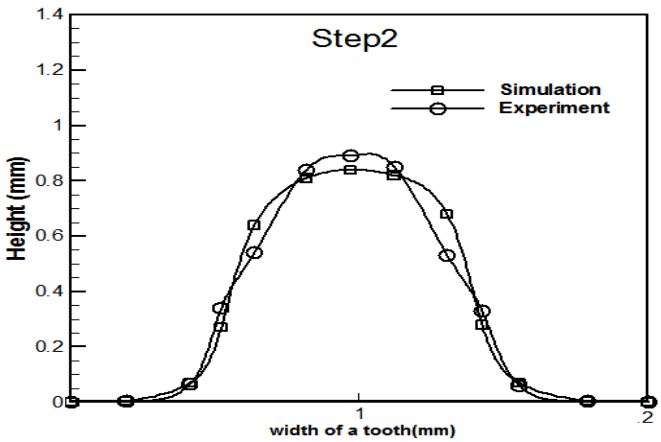

Fig. 13. Tooth shape and height in the second step in both experimental and simulation procedure.

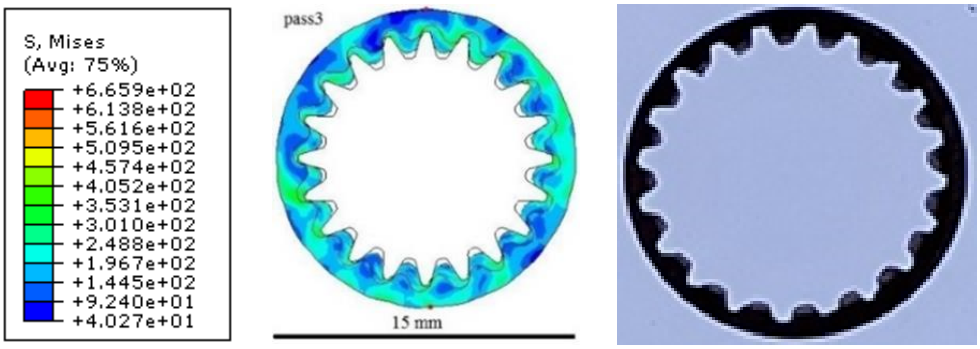

a b c

Fig. 14. Tooth formation in the third step, a) Mises stress b) simulation c) experiment.

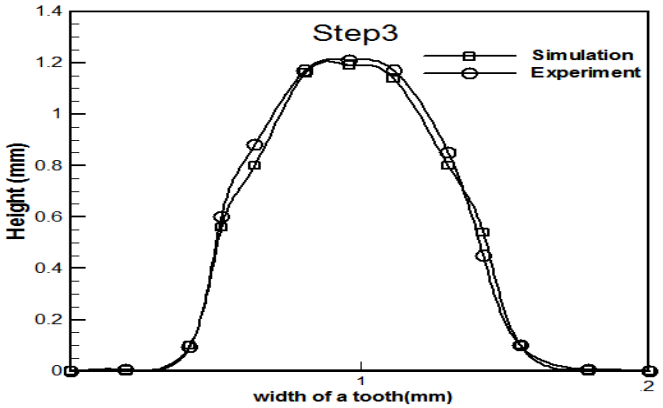

Fig. 15. Tooth shape and height in the third step in both experimental and simulation procedure.

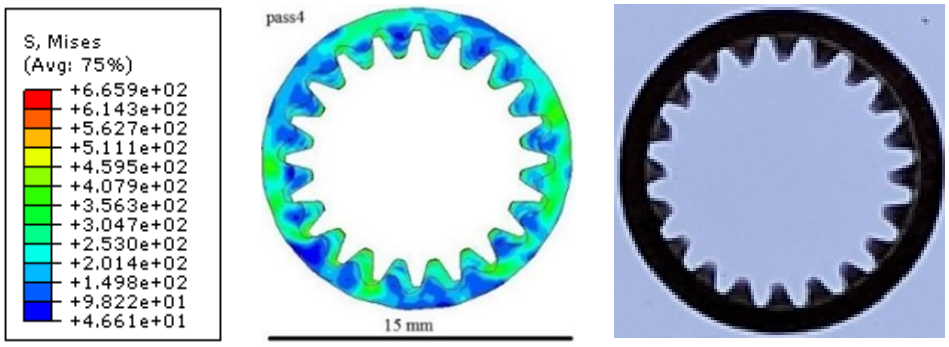

a b c

Fig. 16. Tooth formation in the fourth step, a) Mises stress b) simulation c) experiment.

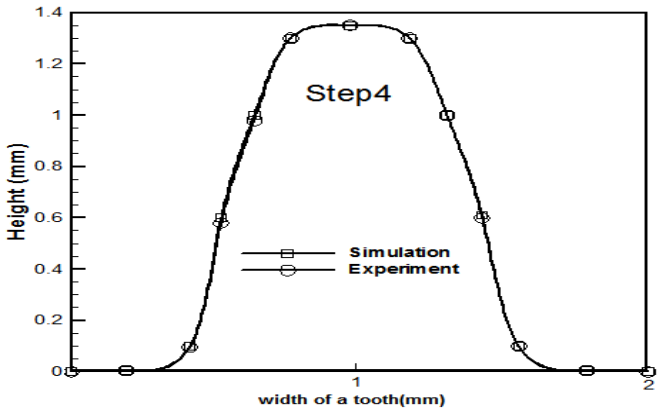

Fig. 17. Tooth shape and height in the fourth step in both experimental and simulation procedure.

5.2. Effective parameters

When the simulation was carried out and the force was obtained for each test, the method of analysis of variance (ANOVA) is used to analyze the test data. The ANOVA results as presented in Table 2. Normality of data distribution was investigated and confirmed using residual normal probability plot. Fig. 18 shows the residual distribution for the process force, which confirms the normality of data distribution. A significance level of 95% was selected meaning that the results are correct with a confidence level of 95%. Therefore, a parameter is significant if the P-value is less than 0.05. According to Table 2, all parameters and interactions are significant and affect the process force except D×T. According to the ANOVA table and eliminating non-effective parameters, the coded regression equation of the process force was developed regarding input parameters in accordance with the model (Equation 1). In this analysis, R-Sq = 99.84 and R-Sq(adj) = 99.69 confirming the ultra-high accuracy of the model, which was developed using the response surface method. To investigate the influences of effective parameters on the process force, the main effects and interactions should be investigated precisely. In this section, the influence of each parameter will be discussed. In the analysis of interactions, other parameters were considered in a balanced mode (central point) of the tests.

$$force = -4119 + 129.70\ D + 74.2\ T + 12979\ f + 59.31\ \alpha - 2.3328\ D*D - 1.651\ T*T - 22510\ f* - 0.2003\ \alpha*\alpha + 41.1\ D*f + 1.4619\ D*\alpha + 782.3\ T*f - 0.646\ T*\alpha - 610.1\ f*\alpha \quad (1)$$

Table 2. ANOVA table for process force

Source	DF	Adj SS	Adj MS	F-Value	P-Value
Model	14	9864450	704604	698.86	0.000
Linear	4	5804639	1451160	1439.32	0.000
D	1	338675	338675	335.91	0.000
T	1	4833935	4833935	4794.50	0.000
f	1	548130	548130	543.66	0.000
α	1	83898	83898	83.21	0.000
Square	4	1592377	398094	394.85	0.000
D*D	1	1556105	1556105	1543.41	0.000
T*T	1	48717	48717	48.32	0.000
f*f	1	90560	90560	89.82	0.000
α*α	1	11467	11467	11.37	0.004
2-Way Interaction	6	2467434	411239	407.88	0.000
D*T	1	1106	1106	1.10	0.311
D*f	1	6765	6765	6.71	0.020
D*α	1	341933	341933	339.14	0.000
T*f	1	611915	611915	606.92	0.000
T*α	1	16706	16706	16.57	0.001
f*α	1	1489010	1489010	1476.86	0.000
Error	16	16132	1008		
Lack-of-Fit	10	12473	1247	2.05	0.197
Pure Error	6	3659	610		
Total	30	9880582			

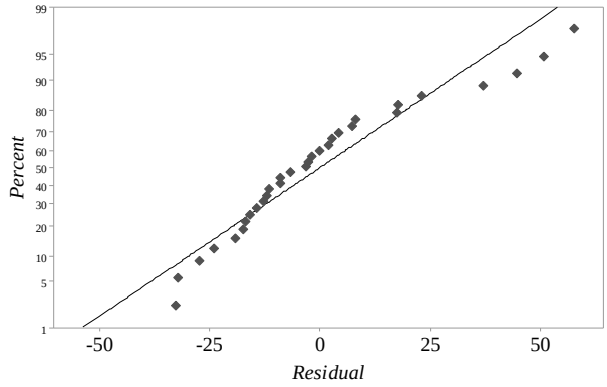

Fig. 18. Normal probability plot of residuals for process force.

5.2.1. Influence of roller diameter

The influence of the roller diameter on the process force is shown in Fig. 19, which indicates that the force increases with increasing the diameter of the roller up to 40 mm and decreases with further increase. By increasing the roller diameter, the area of forming increases and the required force has to be increased to flow the material. When friction increases beyond a specific threshold, temperature increases, recovery takes place, strain hardening decreases and the process force decreases, respectively. Additionally, according to the D×α interaction, which is presented in Fig. 20, the force increases incrementally and then decreases with increasing the roller diameter. However, at large attack angles, the force increases incrementally up to its maximum value because the contact area between the roller and workpiece decreases with increasing the attack angle, which prevents the temperature to be high enough for the recovery. Considering the two diagrams, it is better to use a roller with a small diameter to obtain a lower process force.

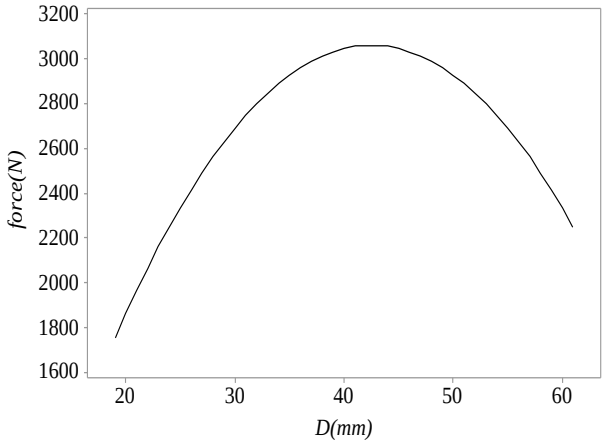

Fig. 19. Main effect plot of roller diameter on process force.

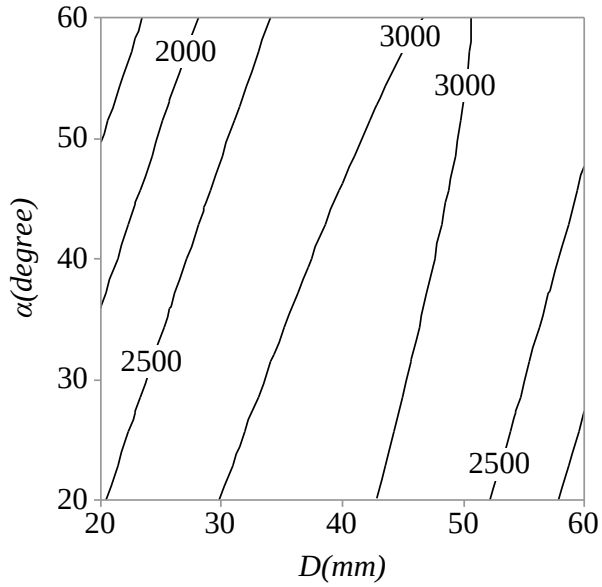

Fig. 20. Interaction plot of roller diameter and attack angle on process force.

5.2.2. Influence of thickness reduction percentage

Given the ANOVA results and coefficients of the regression equations, it can be seen that the thickness reduction percentage has the greatest influence on the process force. According to Fig. 21, which shows the influence of thickness reduction percentage on the process force, the process force rises by increasing the thickness reduction percentage because the deformation zone rises by increasing the thickness reduction percentage meaning that more force is required for the deformation to take place. Moreover, the forming rigidity factor, which is defined according to Equation (2) [18], rises by increasing the thickness reduction percentage, hence leading to an increase in the process force.

$$\text{Forming rigidity} = t/D \qquad (2)$$

In addition, according to the T×f interaction (Fig. 22), the process force rises by increasing the thickness reduction percentage, which is larger in high feed rates. According to the T×α interaction (Fig. 23), the process force rises by increasing the thickness reduction percentage, which is larger at small attack angles. Considering these diagrams, in order to obtain the lowest force value in the process, the lowest thickness reduction ratio should be applied.

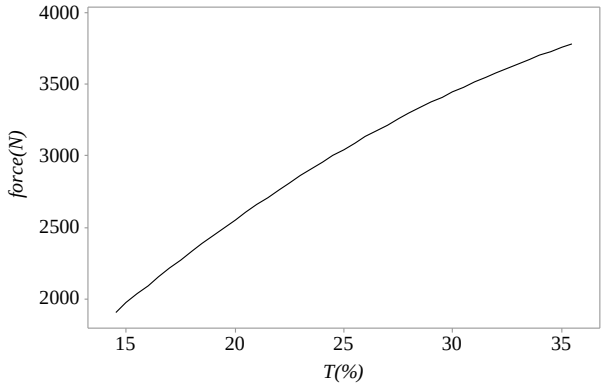

Fig. 21. Main effect plot of thickness reduction percentage on process force.

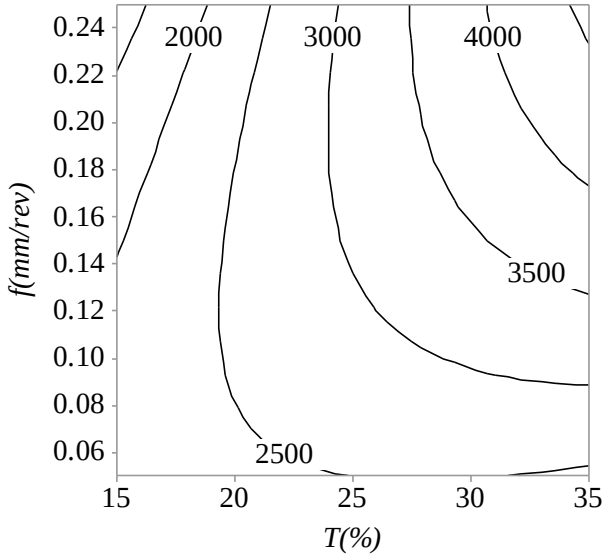

Fig. 22. Interaction plot of thickness reduction percentage and feed rate on process force.

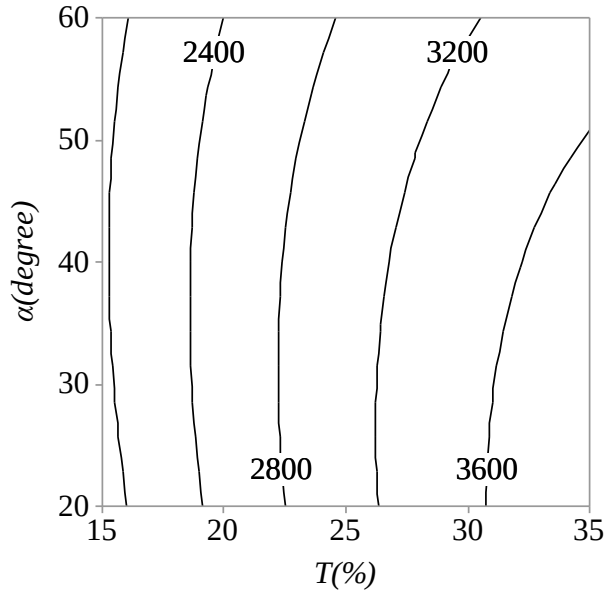

Fig. 23. Interaction plot of thickness reduction percentage and attack angle on process force.

5.2.3. Influence of feed rate

The influence of feed rate on the process force is presented in Fig. 24. As shown in this figure, the process force increases by increasing the feed rate. As the feed rate increases, the rate of deformation and strain rate increases as well, leading to a rise in the deformation stress. Moreover, as the strain rate increases, the exchange temperature of the workpiece with the environment decreases, and the workpiece temperature rises. At high temperatures, the value of m (strain-rate sensitivity of the flow stress) is also significant. As a result, the deformation stress increases, which results in a rise in the process force. The interaction of the thickness reduction percentage and feed rate (Fig. 22) also indicates that the process force rises by increasing the feed rate. In addition, by considering the interaction of f×α, as shown in Fig. 25, the force rises by increasing the feed rate; however, the force decreases a bit by increasing the feed rate at large attack angles. The ratio of tangential to axial contact rises by increasing the feed rate and attack angle, so the sticking friction is the case and the material flow takes place at a lower attack angle in an ultra-large ratio (when both cases take place) and the force decreases, as a result. Considering these diagrams, low feed rates should be used to obtain a lower process force.

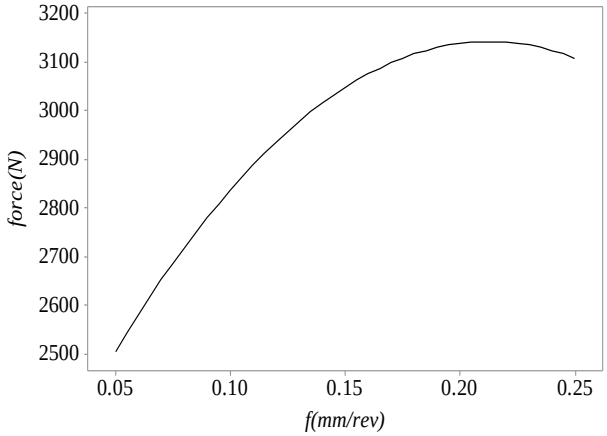

Fig. 24. Main effect plot of feed rate on process force.

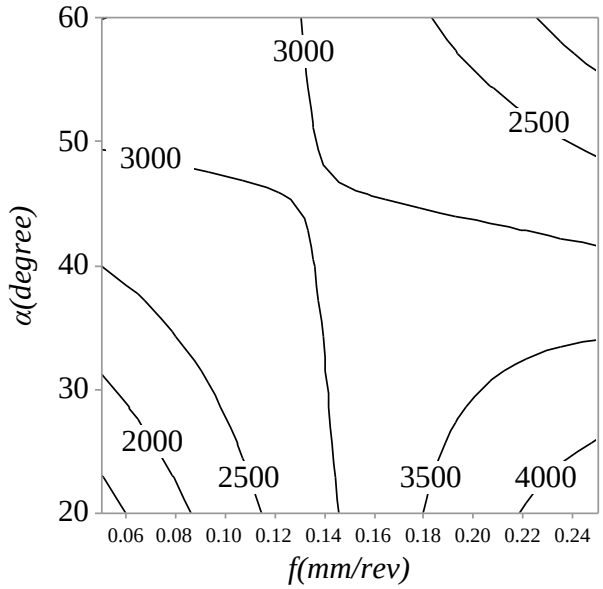

Fig. 25. Interaction plot of feed rate and attack angle on process force.

5.2.4. Influence of attack angle

The influence of the attack angle on the process force is presented in Fig. 26. As can be seen in this figure, the process force decreases by increasing the attack angle because the contact area between the roller and workpiece decreases by increasing the attack angle, leading to a fall in friction and deformation force as well. Due to the interaction of the roller diameter and attack angle, which is presented in Fig. 20, the process force decreases by increasing the attack angle when the roller diameter is less than 40 mm. However, when the roller diameter exceeds 40 mm, the process force rises by increasing the attack angle. This is the result of D×α interaction (discussed in section 5.2.1) and is related to the influence of the roller diameter. In addition, considering the interaction of the thickness reduction percentage and attack angle in Fig. 23, the influence of attack angle on the process force is negligible, and just when the thickness reduction percentage has the maximum value, this influence increases and the process force decreases when the attack angle rises. According to Fig. 25, which presents the interaction of the feed rate and attack angle, the force rises by increasing the attack angle up to a feed rate of 0.15 mm/rev; however, the force decreases by rising the attack angle in higher feed rates, which, as explained in section 5.2.3, is related to the influence of the feed rate. According to these diagrams, the lowest force is obtained with the largest attack angle.

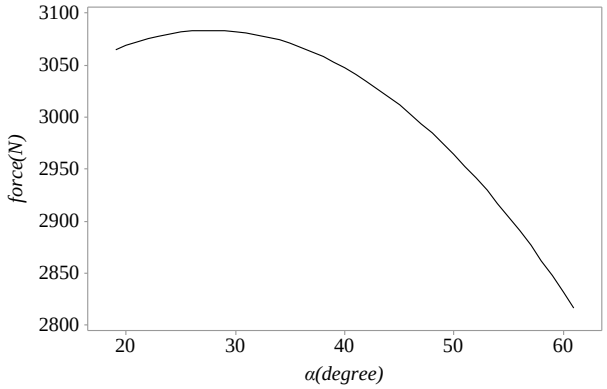

Fig. 26. Main effect plot of attack angle on process force.

6. Conclusion

In the present study, flowforming was used to form an internal gear using a simple setup. The process was also modelled. The model was verified through comparison with experimental results. Some experiments and simulations were carried out to investigate the influence of four process parameters including the roller diameter, feed rate, thickness reduction, and the attack angle on the process force. The analysis of the data using ANOVA revealed that:

- All parameters and interactions are effective on the process force except D×T.
- The force initially rises by increasing the roller diameter up to 40 mm, and then, decreases with a further increase in the diameter.
- Thickness reduction percentage has the strongest influence on the force. The force rises by increasing the thickness reduction percentage.
- The force rises by increasing feed rate.
- The force decreases by increasing the attack angle.

7. References

[1] M. Merklein, J.M. Allwood, B.A. Behrens, A. Brosius, H. Hagenah, K. Kuzman, K. Mori, A. E. Tekkaya, A. Weckenmann, Bulk forming of sheet metal, *CIRP Annals*, 61(2) (2012) 725-745.

[2] C. C. Wong, T. A. Dean, and J. Lin, A review of spinning, shear forming and flow forming processes, *International Journal of Machine Tools and Manufacture*, 43(14) (2003) 1419-1435.

[3] H. Nägele, H. Wörner, and M. Hirschvogel, Automotive parts produced by optimizing the process flow forming–

machining, *Journal of Materials Processing Technology*, 98(2) (2000) 171-175.

[4] P. Groche and D. Fritsche, Application and modelling of flow forming manufacturing processes for internally geared wheels, *International Journal of Machine Tools and Manufacture*, 46(11) (2006) 1261-1265.

[5] S.Y. Jiang, Z.Y. Ren, W. Bin, and G.X. Wu, General issues of FEM in backward ball spinning of thin-walled tubular part with longitudinal inner ribs, *Transactions of Nonferrous Metals Society of China*, 17(4) (2007) 793-798.

[6] S. Jiang, Z. Ren, K. Xue, and C. Li, Application of BPANN for prediction of backward ball spinning of thin-walled tubular part with longitudinal inner ribs, *Journal of materials processing technology*, 196(1-3) (2008) 190-196.

[7] S.Y. Jiang, Y.F. Zheng, Z.Y. Ren, and C.F. Li, Multi-pass spinning of thin-walled tubular part with longitudinal inner ribs, *Transactions of Nonferrous Metals Society of China*, 19(1) (2009) 215-221.

[8] S. Jiang, Z. Ren, C. Li, and K. Xue, Role of ball size in backward ball spinning of thin-walled tubular part with longitudinal inner ribs, *Journal of materials processing technology*, 209(4) (2009) 2167-2174.

[9] M. Haghshenas, M. Jhaver, R. Klassen, and J. Wood, Plastic strain distribution during splined-mandrel flow forming, *Materials & Design*, 32(6) (2011) 3629-3636.

[10] M. Haghshenas, J. Wood, and R. Klassen, Investigation of strain-hardening rate on splined mandrel flow forming of 5052 and 6061 aluminum alloys, *Materials Science and Engineering: A*, 532 (2012) 287-294.

[11] M. Haghshenas, J. Wood, and R. Klassen, Effect of strain-hardening rate on the grain-to-grain variability of local plastic strain in spin-formed fcc metals, *Materials Science and Engineering: A*, 552 (2012) 376-383.

[12]Q.-X. Xia, L.-Y. Sun, X.-q. Cheng, and B.-Y. Ye, Analysis of the forming defects of the trapezoidal inner-gear spinning, in *Industrial Engineering and Engineering Management, 2009. IEEM 2009. IEEE International Conference* (2009) 2333-2337.

[13]W. Xu, X. Zhao, D. Shan, J. Li, Q. Deng, X. Cui, Z. Li, Numerical simulation and experimental study on multi-pass stagger spinning of internally toothed gear using plate blank, *Journal of Materials Processing Technology*, 229 (2016) 450-466.

[14] M. A. Rasouli, A. Taherizadeh, M. Farzin, A. Abdolah, and M. R. Niroomand, Investigating the effects of process parameters on forming forces and defects formation in tube spinning process of AA6061, *Modares Mechanical Engineering*, 16(12) (2017) 186-194.

[15] M. Movahhedy, M. Gadala, and Y. Altintas, Simulation of the orthogonal metal cutting process using an arbitrary Lagrangian–Eulerian finite-element method, *Journal of materials processing technology*,103(2) (2000) 267-275.

[16] D. C. Montgomery, *Design and analysis of experiments*. John wiley & sons, 2017.

[17] C. Wong, T. Dean, and J. Lin, Incremental forming of solid cylindrical components using flow forming principles, *Journal of Materials Processing Technology*, 153 (2004) 60-66.

[18] Y. Jianguo and M. Makoto, An experimental study on paraxial spinning of one tube end, *Journal of Materials Processing Technology*, 128(1) (2002) 324-329.